Journal of Nuclear Materials 390–391 (2009) 1106–1109

Contents lists available at ScienceDirect

Journal of Nuclear Materials

journal homepage: www.elsevier.com/locate/jnucmat

A parameterization of the Lyman α and Lyman β line shapes for radiation transport simulations in divertor plasmas

J. Rosato [a,b,*], D. Reiter [a], H. Capes [b], S. Ferri [b], L. Godbert-Mouret [b], M. Koubiti [b], Y. Marandet [b], R. Stamm [b]

[a] IEF – Plasma Physics, Forschungszentrum Jülich GmbH, Euratom Association, Trilateral Euregio Cluster, D-52425 Jülich, Germany
[b] PIIM, UMR 6633 CNRS – Université de Provence, Centre St. Jérôme, Case 232, F-13397 Marseille Cedex 20, France

ARTICLE INFO

PACS:
32.60.+i
32.70.Jz
47.70.Mc
52.25.Os

ABSTRACT

At high divertor densities as foreseen in ITER, the hydrogen resonance radiation is trapped. This significantly affects the divertor dynamics. The model currently used for photon emission and absorption rates in EIRENE has been improved for the Lyman α and Lyman β lines. All line broadening mechanisms in the atom's rest frame are retained, including Stark, Zeeman and fine structure effects. The influence of the ion dynamics on Stark broadening is described by a computer simulation technique. A parameterization of simulated spectral line shapes is proposed by using a fit subroutine, which allows for fast evaluation of the model in EIRENE.

1. Introduction

Radiation absorption effects have been recognized for a long time in dense and recombining divertor plasmas. In the divertor of Alcator C-Mod, the high gas density (10^{20} m^{-3} and higher) allows very efficient photon absorption at frequencies near the Lyman lines of the hydrogen isotopes, as demonstrated by analyses of line intensity ratio measurements [1] and 2D edge modelling with OSM-EIRENE [2]. Opacity effects are also expected in the ITER divertor plasma because of its large size × density values [3]. Recent simulations with EIRENE for ITER conditions have pointed out the influence of radiation trapping on the plasma ionization – recombination equilibrium. It has been demonstrated that the absorption of photons yields a complex competition between additional ionization and recombination processes: on the one hand, the photon absorption increases the amount of excited atoms, which provides additional ionization; on the other hand, the corresponding extra electron production leads to an increase of the electron density, which entails additional neutral sources by 3-body recombination. Reabsorption is dominated by the Lyman α and Lyman β lines, which respectively contribute to the total photo-ionization source in the plasma edge by about 90% and 10% (see e.g. [4]). Obtaining the best possible accuracy in ionization – recombination equilibrium calculations is a key issue to understand the edge physics in ITER. This paper deals with a set of refinements to the description of radiation transport effects which have very recently been made in EIRENE.

In the code, radiation and neutral transport are treated self-consistently, using the mathematical analogy between the radiative transfer equation and the neutral Boltzmann equation [5]. The source and loss terms for photons are given by rates which strongly depend on the detailed structure of the line shapes. Recently, a computationally efficient model for Lyman α was developed [6], which is based on an analytical calculation of the spectral line profile in the atom's rest frame and retains the Stark and Zeeman effects arising from the interaction between an atom and its environment (electric and magnetic fields). The fine structure was also taken into account. However, the treatment of the Stark effect produced by the ion electric field in the model suffers from uncertainties at high density or low temperature. The latter is described within the frame of the so-called "impact approximation", a model which becomes questionable for Lyman α typically when $N_{e,i} > 10^{14}$ cm^{-3} or $T_{e,i} < 10$ eV. For other Lyman lines, the validity domain shifts towards low density and high temperature as the upper principal quantum number of the transition increases [7]. In this work, we deal with the non-impact regime for Lyman α and Lyman β lines, and provide an easily sampled analytical approximation to their line shapes. We first give a brief presentation of the radiation transport formalism in Section 2, highlighting how the spectral line shape functions appear explicitly in the radiative transfer equation. Next, in Section 3, the Lyman α and Lyman β line shapes in the atom's rest frame are calculated using a numerical simulation technique, which relies on the integration of the time dependent Schrödinger's equation. An estimation of the errors made by using the impact approximation out of its validity conditions is then given. Finally, a parameterization of the simulated line shapes in the regime where the

* Corresponding author. Address: IEF – Plasma Physics, Forschungszentrum Jülich GmbH, Euratom Association, Trilateral Euregio Cluster, D-52425 Jülich, Germany.
E-mail address: j.rosato@fz-juelich.de (J. Rosato).

0022-3115/$ - see front matter © 2009 Elsevier B.V. All rights reserved.
doi:10.1016/j.jnucmat.2009.01.280

impact theory is not applicable, obtained using a genetic algorithm fit subroutine, is presented in Section 4.

2. Radiation transport description

Radiation transport in EIRENE is analogous to a gas of particles (photons) interacting with the surrounding plasma. The fundamental quantity of interest is the "specific intensity" $I_i(\omega,\mathbf{\Omega},\mathbf{r},t)$ [8], which denotes for each line i the energy flux in direction $\mathbf{\Omega}$ per unit of frequency ω and solid angle Ω, at the location $\mathbf{r}$ and time t. This quantity obeys the radiative transfer equation:

$$\left(\frac{1}{c}\frac{\partial}{\partial t}+\mathbf{\Omega}\cdot\nabla+\alpha_i(\omega,\mathbf{\Omega},\mathbf{r},t)\right)I_i(\omega,\mathbf{\Omega},\mathbf{r},t)=S_i(\omega,\mathbf{\Omega},\mathbf{r},t)+\sum_j\int_0^\infty d\omega'\oint d\Omega' K_{ij}(\omega,\mathbf{\Omega};\omega',\mathbf{\Omega}';\mathbf{r},t)I_j\omega',\mathbf{\Omega}',\mathbf{r},t. \quad (1)$$

Here, c denotes the speed of light; $a_i(\omega,\mathbf{\Omega},\mathbf{r},t)$ stands for the loss due to the photon absorption ("extinction coefficient") and is interpreted as the inverse of the photon mean free path; $S_i(\omega,\mathbf{\Omega},\mathbf{r},t)$ is the source related to spontaneous emission; and $K_{ij}(\omega,\mathbf{\Omega};\omega',\mathbf{\Omega}';\mathbf{r},t)$ is the scattering kernel, related to emission in the line i after absorption in the line j, and proportional to the so-called "redistribution function". For the sake of simplicity, the explicit dependence on $\mathbf{r}$ and t will not be written in the following. Presently, the approximation of complete redistribution is made in EIRENE, i.e. the frequency and direction $(\omega,\mathbf{\Omega})$ of the reemitted photon are assumed to be uncorrelated with those of the absorbed photon $(\omega',\mathbf{\Omega}')$. This common approximation allows removal of the scattering kernel from the radiative transfer equation (Eq. (1)) by formally inserting it into the source term S_i. Although this assumption is valid in the case of highly dense plasmas, it should be noted that its reliability has never been quantized in typical divertor plasma conditions. Such a study is now in progress and will be presented in a future work. According to the complete redistribution assumption, the loss and source terms a_i, S_i, are thus given as follows:

$$a_i(\omega,\mathbf{\Omega})=\frac{\hbar\omega_i}{4\pi}B_{lu}N_l\left(1-\frac{g_lN_u}{g_uN_l}\right)\phi_i(\omega,\mathbf{\Omega}), \quad (2)$$

$$S_i(\omega,\mathbf{\Omega})=\frac{\hbar\omega_i}{4\pi}A_{ul}N_u\phi_i(\omega,\mathbf{\Omega}). \quad (3)$$

Here, the subscripts u,l, respectively, stand for the upper and lower energy levels of the atomic transition; N_u, N_l are the related populations with statistical weights g_u, g_l; $\omega_i=\omega_{ul}$ is the Bohr frequency; B_{lu}, A_{ul} are the Einstein coefficients for absorption and spontaneous emission; and the quantity $\phi_i(\omega,\mathbf{\Omega})$ is the line shape function in the laboratory frame with the normalization convention $\int d\omega\, d\mathbf{\Omega}\phi_i(\omega,\mathbf{\Omega})/4\pi=1$. The populations N_u, N_l are treated self-consistently with the radiative transfer equation in EIRENE by a collisional-radiative model. Note that stimulated emission is included in Eq. (1) as a negative contribution to the opacity.

The function $\phi_i(\omega,\mathbf{\Omega})$ is related to the line shape in the atom's rest frame $\phi_i^{at}(\omega,\mathbf{\Omega})$ by a convolution with the neutral velocity distribution function $f(\mathbf{v})$ calculated by EIRENE:

$$\phi_i(\omega,\mathbf{\Omega})=\int dv\, f(v)\,\phi_i^{at}(\omega-\omega_i\mathbf{\Omega}.v/c,\mathbf{\Omega}). \quad (4)$$

An accurate description of the photon absorption and emission rates (Eqs. (2) and (3)) therefore requires to use models for the quantity $\phi_i^{at}(\omega,\mathbf{\Omega})$ which are as accurate as possible. The latter strongly depends on the physical mechanisms which affect an atom, such as the Stark or the Zeeman effects, respectively corresponding to the action of electric and magnetic fields. Its calculation requires a specific treatment founded on the quantum theory of spectral line broadening. In the following section, we introduce this formalism and apply it to the calculation of the Lyman α and Lyman β lines.

3. Line shape modelling

In the theory of line broadening, the line shape in the atom's rest frame is obtained as the Fourier transform of the atomic dipole autocorrelation function $C(t)$. Denoting $\phi_i^{at}(\omega,\mathbf{\Omega})\equiv\phi(\omega)$ thus yields:

$$\begin{cases}\phi(\omega)\propto\frac{1}{\pi}\mathrm{Re}\int_0^\infty C(t)e^{i\omega t}dt\\ C(t)=\sum\limits_{\alpha\alpha'\beta\beta'\varepsilon}d_{\alpha\beta}.\varepsilon(d_{\alpha'\beta'}.\varepsilon)^*\{U_{\alpha'\alpha}(t)U^*_{\beta'\beta}(t)\}\cdot\end{cases} \quad (5)$$

Here, $\mathbf{d}_{\alpha\beta}=\langle\alpha|\mathbf{d}|\beta\rangle$ (resp. $\mathbf{d}_{\alpha'\beta'}=\langle\alpha'|\mathbf{d}|\beta'\rangle$) are transition matrix elements of the atomic dipole operator, between the sublevels α (resp. α′) of the upper level u and the sublevels β (resp. β′) of the lower level l; $\boldsymbol{\varepsilon}$ stands for each polarization vector; $U_{\alpha'\alpha}(t)=\langle\alpha'|U(t)|\alpha\rangle$ and $U_{\beta'\beta}(t)=\langle\beta'|U(t)|\beta\rangle$ are matrix elements of the evolution operator of the emitter $U(t)$; and the brackets {...} denote a statistical average over the perturbing electrons and ions of the plasma, which are assumed to follow a classical path ("semi-classical approximation"). The evolution operator $U(t)$ obeys Schrödinger's equation:

$$i\hbar\frac{dU}{dt}(t)=(H_0-\boldsymbol{\mu}.\mathbf{B}-i\hbar\Phi_e-\mathbf{d}.\mathbf{E}_i(t))U(t), \quad (6)$$

where H_0 is the Hamiltonian of the unperturbed atom which retains fine structure, $-\boldsymbol{\mu}.\boldsymbol{B}$ is the Zeeman effect term ($\boldsymbol{\mu}$ is the emitter's magnetic dipole and $\boldsymbol{B}$ the magnetic field), the non-hermitic term $-i\hbar\Phi_e$ describes broadening of the sublevels by electron collisions ("electron collision operator", see [9]), and $-\boldsymbol{d}.\boldsymbol{E}_i(t)$ is the Stark effect term related to the microscopic electric field $\boldsymbol{E}_i(t)$ which is created by the ions. In the case where the typical time scale of the ion electric field τ_{Ei} is much lower than the inverse of the characteristic line width $1/\Delta\omega_0$, the ion contribution can also be described by a non-hermitic term $-i\hbar\Phi_i$ ("ion collision operator") like the electrons, and equation (6) can be solved analytically. This is the ion impact assumption, which was used in our previous work [6] for the Lyman α line. This assumption has the major advantage to lead to an analytical expression for the line shape. It was shown that the line profile is given by a sum of Lorentzian functions, of which the number, position, intensity and width are the result of a competition between the Stark, Zeeman, and fine structure effects.

However, as already pointed out in the introduction, the impact assumption for ions is only marginally valid for Lyman α in conditions of cold and dense divertor plasmas ($N>10^{14}\,\mathrm{cm}^{-3}$, $T_{e,i}<5$ eV), where the inequality $\tau_{Ei}\ll 1/\Delta\omega_0$ is not fully verified, and becomes less and less valid for the other Lyman lines as the principal quantum number increases [7]. The size of the error made using the impact model is given in Fig. 1 for Lyman α and in Fig. 2 for Lyman β with the conditions $N=5\times10^{14}\,\mathrm{cm}^{-3}$, $T_{e,i}=1$ eV, $B=5$ T, and $\theta=(\boldsymbol{B},\mathbf{\Omega})=90°$ ($\Delta\omega$ denotes the frequency detuning). The line shapes obtained with the analytical impact model have been compared to those obtained by the numerical simulation technique. The latter provides reference profiles, since it consists in ab initio numerical calculations of the dipole autocorrelation function in term of simulated histories of the electric field [10]. In each figure, the profile presents the structure characteristic to Zeeman effect in the strong field regime (Paschen-Back effect), i.e. a splitting of the line into one central component and two lateral doublets (here overlapped in the case of Lyman β). However, significant discrepancies are visible, in particular on the central component. A rough estimation shows that the impact assumption overestimates the line width by a factor of about 2. This is the consequence of the non-impact effects mentioned above.

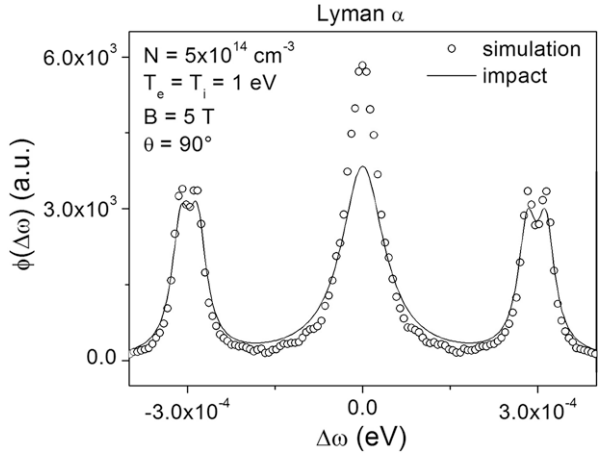

Fig. 1. Profile of Lyman α line, obtained using the impact approximation (solid line) and the numerical simulation method (circles), with the conditions $N = 5 \times 10^{14}$ cm^{-3}, $T_e = T_i = 1$ eV, $B = 5T$, and $\theta = 90°$. The impact model significantly overestimates the width of the central component. Here, a splitting of the lateral components into fine structure doublets is visible.

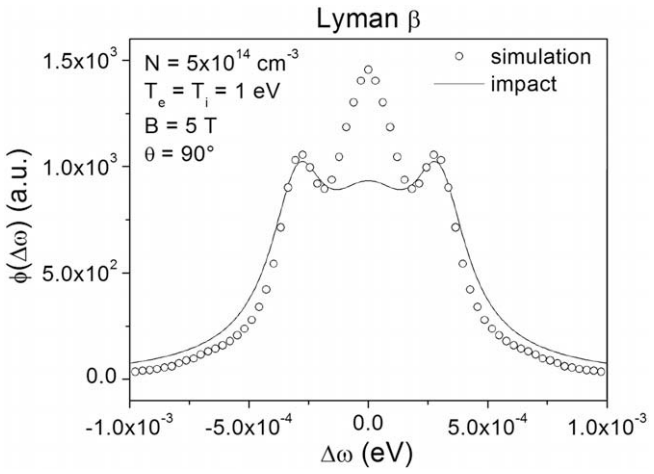

Fig. 2. The same plot as in Fig. 1, here for Lyman β line.

As a result of this investigation, it is clear that using the results of the numerical simulation technique is required for an accurate description of the line shapes in our conditions of interest. In practice, however, it is not realistic to implement such an ab initio calculation into EIRENE since this technique is CPU intensive. In the following, we present a parameterization of a set of simulated profiles, obtained using a fitting routine.

4. Adjustment of profiles for implementation into EIRENE

A multi-Lorentzian model, taking into account the Paschen – Back structure presented above, has been fitted to simulated Lyman α and Lyman β profiles. The model is defined by:

$$\phi(\Delta\omega) = K_0 L_{\gamma_0}(\Delta\omega) + K_1[L_{\gamma_1}(\Delta\omega - \omega_{++}) + L_{\gamma_1}(\Delta\omega - \omega_{+-}) + L_{\gamma_1}(\Delta\omega - \omega_{-+}) + L_{\gamma_1}(\Delta\omega - \omega_{--})]. \quad (7)$$

Here, $L_a(x) = (a/\pi)/(x^2+a^2)$ stands for the normalized Lorentzian function; γ_0, γ_1 are respectively the widths of the central and lateral components and are set as adjustable parameters; $K_0 = (\sin^2\theta)/2$ and $K_1 = (1+\cos^2\theta)/8$ are amplitude factors which depend on the angle $\theta = (\boldsymbol{B},\boldsymbol{\Omega})$ between the direction of the magnetic field and the photon propagation direction; $\omega_{\varepsilon_1\varepsilon_2} = \varepsilon_1\ \omega_Z + \varepsilon_2\ \omega_{fs}$ $(\varepsilon_{1,2} = \pm 1)$ are

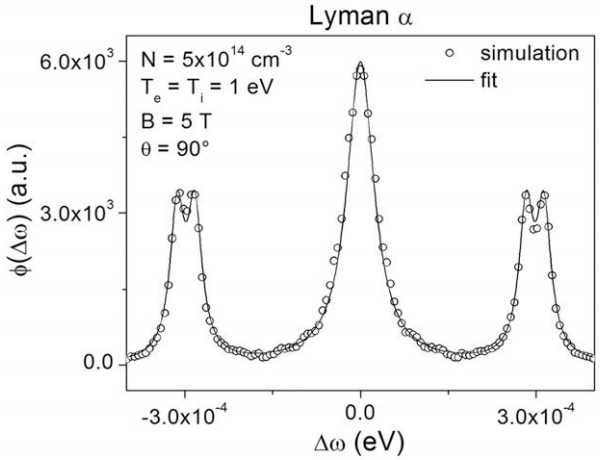

Fig. 3. The model (solid line) provides a very good fit to the result of numerical simulations (circles).

frequencies of the lateral components, which depend both on Zeeman and fine structure spin-orbit frequencies $\omega_Z = eB/2m_e$ and $\omega_{fs} = \alpha^2 \mathrm{Ry}/6\hbar n^3$ (here α is the fine structure constant and Ry is the Rydberg energy). We have performed the fits with a χ^2 minimization routine, using the genetic algorithm "PIKAIA" [11] on a density range from 10^{14} cm^{-3} to 10^{15} cm^{-3}, and assuming fixed values for the temperatures, namely $T_{e,i} = 1$ eV. The model has been found to reproduce the simulated profiles very well in the whole range of density considered. An example of these results is reported in Fig. 3, where a fit of Lyman α profile is plotted in the case where $N = 5\text{x}10^{14}$ cm^{-3}. In the whole range of density, the central and lateral widths have been found to be roughly proportional to those obtained using the impact approximation. This allows for easy implementation of the non-impact effects on the photon emission and absorption rates into EIRENE. We have estimated the ratios ${\gamma_0}^{\mathrm{fit}}/{\gamma_0}^{\mathrm{imp}}$ and ${\gamma_1}^{\mathrm{fit}}/{\gamma_1}^{\mathrm{imp}}$ between the impact and the fit widths as respectively equal to 0.67 and 0.94 for Lyman α, and equal to 0.55 and 0.93 for Lyman β.

5. Conclusion

We have performed a parameterization of simulated Doppler free Lyman α and Lyman β line shapes of the hydrogen isotopes in the typical density range found in divertor plasmas. All line broadening mechanisms are retained, such as the Zeeman, Stark, and fine structure effects. The Stark effect has been described by using the numerical simulation technique, which provides reference profiles when the impact assumption is not valid for the ions. This is precisely the case in highly dense divertor plasmas like in Alcator C-Mod. Calculations of the ionization – recombination equilibrium retaining the line shape parameterization are being now performed with EIRENE. These should eventually allow quantification of the role of non-impact effects on the photon absorption and emission rates. An extension of this work would consist in developing the same kind of adjustment in terms of the temperature and/or the magnetic field. Further work could also consist of lines with higher principal quantum number. This could even be applied in a diagnostic purpose, for example to the Balmer lines commonly used in spectroscopy measurements.

Acknowledgements

This work is partially supported by a Euratom mobility contract and by the project "Radiation absorption effects" of the fédération de recherche sur la fusion par confinement magnétique, in the frame of the LRC DSM 99-14 (Laboratoire PIIM / CEA Cadarache).

References

[1] J.L. Terry et al., Phys. Plasmas 5 (1998) 1759–1766.
[2] S. Lisgo et al., J. Nucl. Mater. 337–339 (2005) 139–145.
[3] A. Loarte et al., Nucl. Fus. 47 (2007) S203–S263.
[4] V. Kotov et al., Contrib. Plasma Phys. 46 (2006) 635–642.
[5] D. Reiter et al., J. Nucl. Mater. 363–365 (2007) 649–657.
[6] J. Rosato et al., J. Nucl. Mater. 363–365 (2007) 421–425.
[7] J. Rosato et al., Contrib. Plasma Phys. 48 (2008) 153–157.
[8] D. Mihalas, Stellar Atmospheres, W.H. Freeman and Company, San Fransisco, 1978.
[9] H.R. Griem, A.C. Kolb, K.Y. Shen, Phys. Rev. 116 (1959) 4–16.
[10] R. Stamm, E.W. Smith, B. Talin, Phys. Rev. A 30 (1984) 2039–2046.
[11] P. Charbonneau, Astrophys. J. Suppl. Ser. 101 (1995) 309–334.